

# Protect Federated Learning Against Backdoor Attacks via Data-Free Trigger Generation

Yanxin Yang<sup>1</sup>, Ming Hu<sup>2\*</sup>, Cao Yue<sup>2</sup>, Jun Xia<sup>1</sup>, Yihao Huang<sup>2</sup>, Yang Liu<sup>2</sup>, Mingsong Chen<sup>1\*</sup>

<sup>1</sup>MoE Engineering Research Center of SW/HW Co-Design Tech. and App., East China Normal University, China

<sup>2</sup>School of Computer Science and Engineering, Nanyang Technological University, Singapore

**Abstract**—As a distributed machine learning paradigm, Federated Learning (FL) enables large-scale clients to collaboratively train a model without sharing their raw data. However, due to the lack of data auditing for untrusted clients, FL is vulnerable to poisoning attacks, especially backdoor attacks. By using poisoned data for local training or directly changing the model parameters, attackers can easily inject backdoors into the model, which can trigger the model to make misclassification of targeted patterns in images. To address these issues, we propose a novel data-free trigger-generation-based defense approach based on the two characteristics of backdoor attacks: i) triggers are learned faster than normal knowledge, and ii) trigger patterns have a greater effect on image classification than normal class patterns. Our approach generates the images with newly learned knowledge by identifying the differences between the old and new global models, and filters trigger images by evaluating the effect of these generated images. By using these trigger images, our approach eliminates poisoned models to ensure the updated global model is benign. Comprehensive experiments demonstrate that our approach can defend against almost all the existing types of backdoor attacks and outperform all the seven state-of-the-art defense methods with both IID and non-IID scenarios. Especially, our approach can successfully defend against the backdoor attack even when 80% of the clients are malicious.

## I. INTRODUCTION

Federated Learning (FL) [1]–[4] as a promising distributed machine learning paradigm, enables multiple clients to collaboratively train an Artificial Intelligence (AI) model without sharing their raw data. Because of the advantages in privacy protection, FL is widely used in medical care systems [5], autonomous driving [6], and IoT systems [7], [8]. However, due to the lack of data auditing for untrusted clients, the conventional FL methods are susceptible to poisoning attacks, particularly to the backdoor attack [9]–[11]. Using specific poisoned datasets, the attacker can make the model learn a targeted misclassification functionality. By embedding specialized patterns (i.e., *triggers*) into the input, the attacker can control the model to misclassify into a target category. Since it will not cause a degradation of the model inference accuracy on clean data, the backdoor attack has a strong concealment [12]–[14]. In FL, the clients are large-scale and independent, it is difficult to guarantee that all the clients are trustworthy. By uploading poisoned models for aggregation, these untrustworthy clients, called adversarial clients, can easily inject backdoors into the global model. Furthermore,

attackers can set different learning rates or directly modify the model parameters to intensify their attacks. Although there are various backdoor defense methods in traditional deep learning [15]–[18], most of them need to retrain the model with additional auxiliary datasets or access to the training data [19]. However, since the raw data of each client is inaccessible, data-dependent defense methods are difficult to perform in FL.

In order to defend against backdoor attacks on FL, various methods have been proposed, which can be classified into two categories, i.e., similarity-based methods [20]–[22] and Differential Privacy (DP)-based methods [23], [24]. However, these methods all have their shortcomings and limitations. Similarity-based methods are limited by the data distribution, when the data on clients are not independent-and-identically-distributed (non-IID), the effect of these methods will be reduced or even completely invalid. For DP-based methods, using noise to mitigate backdoors inevitably leads to a degradation of the model inference accuracy. Therefore, how to defend against backdoor attacks on FL without additional datasets or prior knowledge and ensure that the accuracy of the task does not degrade in different data distribution scenarios is becoming a great challenge.

To address the above challenge, we propose a novel data-free trigger-generation-based approach to defend against backdoor attacks in FL. Our approach is motivated by several observations [18], [25]–[27] indicating that: i) backdoor tasks are easier than normal classification tasks to train, and ii) the model learns trigger knowledge faster than learning normal classification knowledge. Therefore, in our approach, we use Conditional Generative Adversarial Networks (CGAN) [28] to extract the new knowledge gained in the current FL round from the aggregated global model in the form of images. For each category, our CGAN generates an image, which could not be classified by the global model of the previous round, but can be classified into the corresponding category by the current global model. In this way, each image contains newly learned knowledge for a specific category. These images will also include the knowledge of triggers if the global model is backdoored. However, merely utilizing these generated images to filter the poisoned models is insufficient, other knowledge present in the images, aside from the backdoor, may mistakenly eliminate benign clients, resulting in reduced accuracy performance and slower convergence, particularly in Non-IID scenarios. Therefore, our approach aims to generate

\* Ming Hu and Mingsong Chen are corresponding authors. Email: hu.ming@ntu.edu.sg and mschen@sei.ecnu.edu.cn

the images containing only trigger knowledge. We design the mechanism according to the properties of the backdoor that the poisoned model can be manipulated to misclassify images embedded triggers with a high degree of confidence [12]–[14]. Intuitively, our approach strives to generate a trigger image for each category, ensuring that when this image overlaps with the previous generated images, all of them are misclassified into the target category. By using these trigger images, the server can eliminate poisoned models and aggregates the remaining local models to get the benign global model. This paper makes three major contributions as follows:

- We propose a novel approach to defend against backdoor attacks in FL that utilizes trigger generation to detect and eliminate poisoned models without using any prior knowledge and auxiliary datasets.
- We design the knowledge extraction and trigger filtering mechanism to identify poisoned models, where trigger filtering improves the generalization and reliability of our approach in cases of extreme data distribution heterogeneity.
- We conduct various experiments on four well-known datasets with varying data distributions, which shows that our approach can prevent backdoor attacks to the greatest extent possible without sacrificing the accuracy of the main task.

## II. RELATED WORK

**Backdoor Attacks on FL** Backdoor attacks on FL [9]–[11], [29] can be classified into two categories according to their frequency of occurrence: single attacks and multiple attacks. In the case of multiple attacks, when the adversarial clients are selected by the server, they attempt to inject backdoors into their local models and upload these models to participate in the aggregation. Although a few attacks may not significantly impact the global model, the backdoor will be subtly injected into the global model over time. Therefore, this attack type usually has a prolonged time span and is relatively concealed, but it requires the attacker to control a significant number of clients, which is a disadvantage and limitation.

On the other hand, for single attacks, the attacker aims to successfully inject the backdoor through a single attack. However, the disadvantage of this attack type is that the attack process often involves scaling up the uploaded model parameters to maximize the impact during aggregation, which leads to a reduction in the concealment of the attack. In response to this feature, defenses can easily identify models with parameters that are significantly larger than normal parameters and exclude them from the aggregation process [23]. Additionally, since FL continues to train with the benign data after the attack, the effect of the attack may gradually decrease, in light of which, some methods [11], [29] proposed improvement measures.

**Backdoor Defenses on FL** The mainstream backdoor defenses in FL approaches can be classified into two major categories. The first type is similarity-based methods [20]–[22], [30]. These methods aim at eliminating poisoned models

with low similarity to other models [20] or avoid aggregating abnormal model parameters by changing the aggregation strategy [21], [22]. The second type is Differential Privacy (DP)-based methods [23], [24]. These methods involve injecting a sufficient amount of noise into the global model to eliminate the effects of backdoor attacks. However, these defense methods have significant limitations. For similarity-based methods, it becomes difficult to detect poisoned models when the data on clients are not independent-and-identically-distributed (non-IID), the reason is that different distributions of local datasets also cause the updated models to be less similar to the others, which makes these models difficult to be distinguished from poisoned models. Furthermore, the anomaly detection algorithm based on similarity loses its effectiveness when numerous adversarial clients participate in the same round, or when the number of adversarial clients is too large. Meanwhile, DP-based methods have limitations since the specific amount of added noise is challenging to be determined. In order to ensure the effectiveness of the defense, more noise will be added, which leads to a decline in the accuracy of model inference.

To the best of our knowledge, our approach is the first to use CGAN to generate backdoor triggers in FL without any prior knowledge or auxiliary datasets. Our approach is designed based on the characteristics of backdoor triggers, rather than similarities between models. Therefore, it remains applicable in non-IID scenarios of FL and keeps effective when the majority of clients are adversarial.

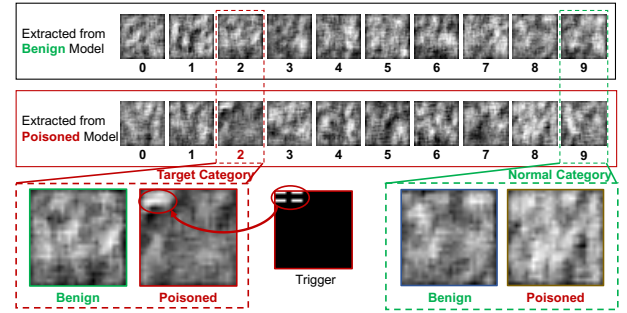


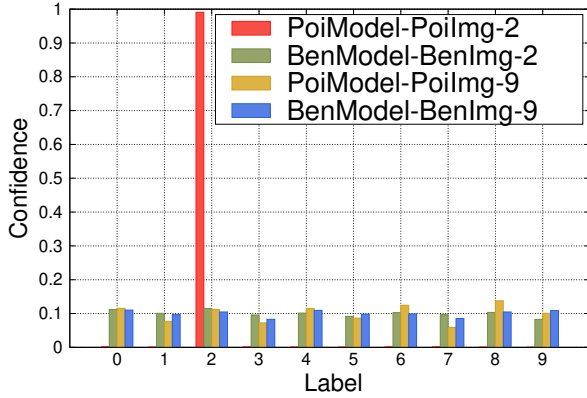
Fig. 1. Generated images and the trigger.

## III. MOTIVATION

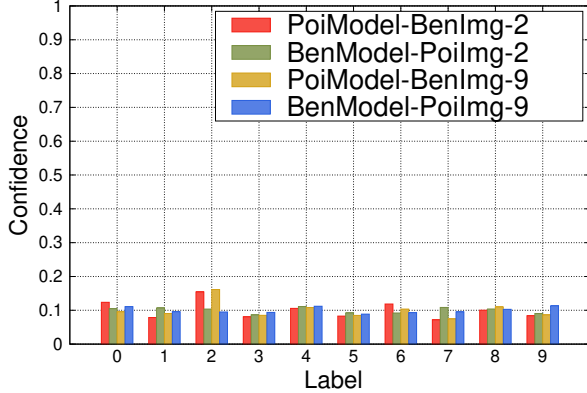
There are various recent works [18], [25]–[27] observed that compared to the normal task, the backdoor task is much easier to train, and in the early stage of model training, the training loss of the backdoor task drops faster than the normal task. Intuitively, in each round of the early training stage, the model can learn more knowledge of backdoor triggers compared to the normal classification knowledge. Inspired by this intuition, we attempt to generate the newly learned knowledge of the current model by using CGAN. In specific, we select a trained model  $m_0$  for the classification task of MNIST dataset and retrain this model using clean data and poisoned data for one more round, respectively. In this way,

we obtain a benign model  $m_b$  and a poisoned model  $m_p$ . Note that here the backdoor target category is “2”. Then, we use CGAN to generate an image for each category, where the optimal goals of CGAN are that let the generated images i) cannot be classified by  $m_0$  and ii) can be classified into each category by the models respectively. (i.e.,  $m_b$  or  $m_p$ ). In this way, we can extract the newly learned features of each category from  $m_b$  and  $m_p$ .

**Observation 1.** Figure 1 presents the generated images and the backdoor trigger. From Figure 1, we can observe that the image for the backdoor target category (i.e., “2”) from the poisoned model includes patterns of the trigger, while the images from the benign model do not include. In addition, we can also observe that the images for the other normal categories from both benign and poisoned models do not include the trigger. Therefore, the learned trigger knowledge can indeed be easily generated by CGAN.



(a) Inference

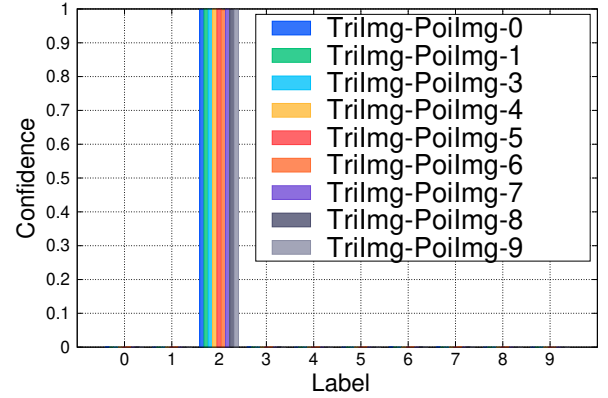


(b) Cross-inference

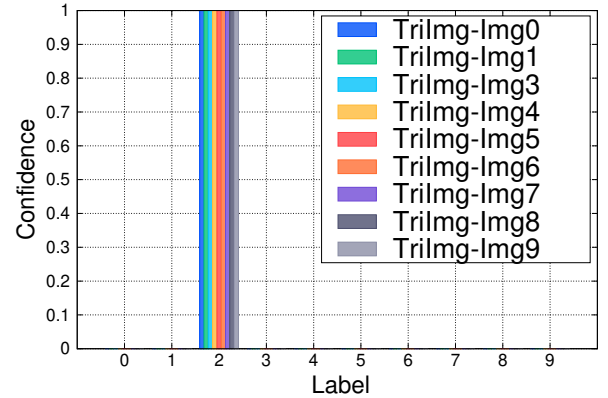
Fig. 2. Outputs of poisoned and benign model for generated images.

**Observation 2.** To explore the impacts of the extracted normal and trigger knowledge on model inference, we use both  $m_b$  and  $m_p$  to infer all the generated images. Figure 2 presents the outputs of the poisoned and benign model for the generated images for categories “2” and “9”. Here notations “PoiModel” and “BenModel” denote the poisoned model and the benign model, respectively. Notations “PoiImg- $x$ ” and “BenImg- $x$ ”

denote the image generated from the poisoned model and the benign model for category “ $x$ ”, respectively. Note that since the target category of the poisoned model is “2”, the “PoiImg-9” only includes normal knowledge. In Figure 2(a), the poisoned and the benign model infer the images generated from themselves. Conversely, in Figure 2(b), they infer the images generated from each other. From Figure 2, we can observe that the image with the trigger can be clearly classified to the target category on the poisoned model, but it only makes an ambiguous classification result on the benign model. We can also find that neither the poisoned model nor the benign model can clearly classify the images with normal knowledge. Based on these observations, we can find that compared with the normal knowledge, the extracted trigger can significantly affect the inference of the poisoned model.



(a) Generated Images



(b) Data Samples

Fig. 3. Inference outputs of images overlapped with the generated trigger.

**Observation 3.** To explore the capability of the generated trigger to change classification, we overlap the generated trigger image (i.e., “TriImg”) with all the other generated images and data samples (e.g., “Img $x$ ” for category  $x$ ) for each category. Figure 3 presents the inference results of all the overlapped images using the poisoned model. From Figure 3, we can observe that the generated trigger can make the poisoned model misclassify all the overlapped images into the target category. Therefore, the generated trigger can achieve a

similar capability as the original backdoor triggers. Figure 4 presents the inference results of data samples overlapped with the sample of category 2. We can find that the poisoned model cannot clearly misclassify all the overlapped images into category 2. Therefore, the generated trigger can achieve a better capability than the normal knowledge to change classification.

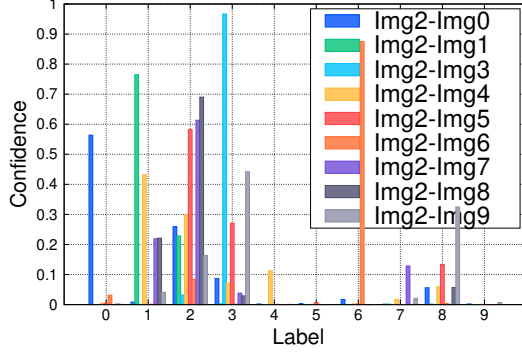


Fig. 4. Inference outputs of data samples overlapped with the sample of category 2.

**Our Idea.** Inspired by the above observations, we present a novel trigger generation-based defense approach against backdoor attacks for FL. In specific, inspired by Observation 1, in each round of FL, we can extract the newly learned knowledge for each category of the global model by comparing with the old version global model. Inspired by Observation 2, by using both the current and the old version global model to infer the generated images, we can identify potential triggers from generated images. Inspired by Observation 3, by generating the images that can change the classification result when overlapping them on other images, we can precisely get the knowledge of backdoor triggers. By eliminating local models that can clearly classify the generated backdoor triggers into their category, we can defend against backdoor attacks in FL.

#### IV. OUR APPROACH

##### A. Problem Setup

**Adversary Capability** We assume that the attacker controls a subset of participating clients, referred to as adversarial clients. The attacker has complete control over these clients, which enables them to launch attacks without complying with any specified hyperparameter of FL, such as training epochs and learning rate. Moreover, the adversarial clients can directly manipulate the model’s parameters to be uploaded, thereby achieving the attack objective. The attacker has the discretion to determine whether the adversarial clients will conduct an attack or not upon selection. The adversarial clients can collaborate with one another under the attacker’s guidance to enhance the overall effectiveness of the attack. However, it is important to note that the attacker cannot control or influence the benign clients or the server’s aggregation process.

**Evaluation Criteria** When assessing the effectiveness of a backdoor attack, two criteria are commonly used: Main

task Accuracy (MA) and Attack Success Rate (ASR), which respectively measure the stealthiness and strength of the attack. The attack succeeds if the poisoned model outputs the backdoor target classes when the trigger patterns are added to the input images. The attacker aims to achieve a similar MA to that of the FL system without being attacked, while simultaneously achieving a higher ASR. On the other hand, the defender aims to reduce the ASR as much as possible while minimizing the impact on the MA.

##### B. Overview

Figure 5 presents the workflow of our defense approach. As shown in Figure 5, all the key components of our defense approach are deployed on the cloud server and our approach does not require any additional data. Similar to the traditional FL, in our approach, the server first randomly selects  $N$  clients and dispatches the current global model to them, where  $N$  is the number of selected clients in each FL round. The clients then utilize their raw data to train the models and updated the trained models to the server. However, due to existing adversarial clients participating in local training, there may exist poisoned models in the uploaded models. For example, in Figure 5, *Client#2* is an adversarial client, and it uploads a poisoned model to the server. To defend against backdoor attacks, as shown in Figure 5, our approach consists of three stages, i.e., knowledge extraction, trigger filtering, and model filtering, respectively. Let  $G_{old}$  denote the dispatched global model and  $G_{agg}$  indicate the aggregation model of all the uploaded models. In specific, these three stages are introduced as follows:

- **Stage 1: Knowledge extraction** is performed to generate images for each category, denoted as the set  $I$ . These images contain the knowledge about the differences between the two global models, i.e.,  $G_{old}$  and  $G_{agg}$ . Additionally, if any of the models are poisoned, the  $I$  images also capture the information about triggers.
- **Stage 2: Trigger filtering** is applied to identify key knowledge from the  $I$  images that can cause significant changes in classification. This process generates the possible trigger images for each category, denoted as the set  $T$ .
- **Stage 3: Model filtering** utilizes the  $T_{Gen}$  images to detect any poisoned models in the set  $M$  and re-aggregates the remaining benign models. The resulting aggregated global model is then sent out in the next round of FL.

##### C. Knowledge Extraction

The first stage of our approach, knowledge extraction, is predicated on the assumption that previous FL defenses have been effective, so that the current global model  $G_{old}$  is benign, which means there is no knowledge about triggers in  $G_{old}$ . This stage aims to generate images for each category that highlight the differences between  $G_{old}$  and the new aggregated global model,  $G_{agg}$ . Importantly, if any models have been attacked, the generated images will also contain the knowledge about the triggers. To achieve this, we leverage the Conditional

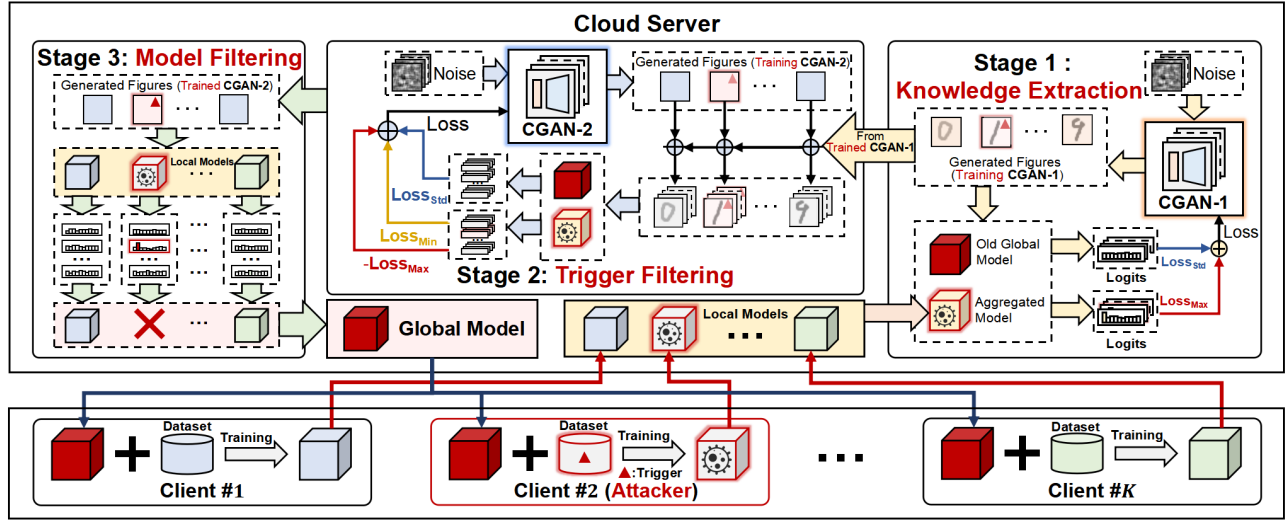


Fig. 5. Workflow of our approach

Generative Adversarial Network (CGAN) [28] and develop the algorithm outlined in Algorithm 1.

**Algorithm 1: Knowledge Extraction**

**Input:** i)  $G_{old}$ , old global model; ii)  $G_{agg}$ , new global model; iii)  $E$ , training rounds; iv)  $C$ , category number; v)  $\gamma$ , balance coefficient;

**Output:**  $I_{Gen}$ , set of generated images;

```

1  $D1 \leftarrow G_{old}$ 
2  $D2 \leftarrow G_{agg}$ 
3  $Gen \leftarrow random$ 
4  $z \leftarrow noise$ 
5  $label \leftarrow \{0, 1, \dots, C - 1\}$ 
6 for  $epoch=0$  to  $E$  do
7    $Imgs \leftarrow Gen(z, label)$ 
8    $Loss \leftarrow 0$ 
9   for  $c=0$  to  $C$  do
10     $img \leftarrow Imgs(c)$ 
11     $Loss_{std} \leftarrow std(D1(img))$ 
12     $Loss_{max} \leftarrow 1 - D2(img, c)$ 
13     $Loss \leftarrow \gamma \times Loss_{std} +$ 
       $(1 - \gamma) \times Loss_{max} + Loss$ 
14   end
15   Update  $Gen$  by  $Loss$ 
16 end
17  $I \leftarrow Gen(z, label)$ 

```

At the start of the algorithm, Lines 1-5 depict the initialization phase. In our CGAN, two discriminant networks, namely  $D_1$  and  $D_2$ , are utilized. These networks are initialized with the respective parameters of  $G_{old}$  and  $G_{agg}$ . In Line 3, we initialize the  $Gen$  randomly as the generation network, which has two inputs, namely  $z$  and  $label$ . The  $z$  input is a set of  $C$  random noises vectors that are used to enrich the diversity of the generated images, each of which has a length of the

dimensionality of the latent space, where  $C$  denotes the total number of categories in the dataset. The  $label$  input is a vector of integers from 0 to  $C$ . Starting from Line 6, we loop  $E$  times to train the generation network  $Gen$ . Line 7 shows that we use  $Gen$  to generate the images set  $Imgs$ , the length of which is also  $C$ . In order to train  $Gen$ , we design the loss function, as shown in Lines 10–13 of the Algorithm 1.

For each item in the  $Imgs$ , denoted as  $img = Imgs(c)$ , we need to accumulate its loss value as Line 13 of the algorithm, where  $\gamma$  is a hyperparameter that balances the two terms in the loss function. The first term of the loss function,  $Loss_{std}$  in Line 11 of the Algorithm 1, aims to minimize the standard deviation (std) of the probability distribution of the generated image,  $img$ , across all categories, as evaluated by  $D_1$ . This encourages the generated image to be ambiguous and difficult to  $D_1$  to classify. The second term of the loss function,  $Loss_{max}$  in Line 12, aims to maximize the probability of the generated image,  $img$ , being classified as the current category  $c$ , by  $D_2$ , which encourages the generated image to have a clear classification result for  $D_2$ . Through optimization of the Loss function, we can get the trained  $Gen$  which generates the images that exhibit completely distinct classification tendencies when inputted into  $G_{old}$  and  $G_{agg}$ , respectively. As  $G_{agg}$  is aggregated by the local models trained from  $G_{old}$ , we can assume that the generated images are indicative of the new knowledge learned by the FL system in this round. Ultimately, in Line 17, we save the generated images for all categories, yielding the image set  $I$ .

**D. Trigger Filtering**

Though the images generated in Stage 1,  $I$ , may contain the knowledge about triggers, these images cannot be directly used for eliminating models. This is because, during the early and middle phases of convergence in FL training,  $G_{agg}$  will acquire a substantial amount of new normal knowledge



compared to  $G_{old}$ , which will also be incorporated into  $I$ . The extreme non-IID data distribution in FL can also result in similar outcomes. This additional normal knowledge can significantly affect the eliminating process of models, leading to missed calls or misjudgments in determining whether the model is poisoned, resulting in defense mechanism failure, a slow convergence rate, or even a complete failure to converge. Therefore, the second stage of our approach, trigger filtering, aims to filter from  $I$  to get more precise trigger knowledge that can significantly alter the image classification results, to avoid the interference of the other normal knowledge. Similar to the first stage, we utilize CGAN to generate trigger images for each category. The algorithm is outlined in Algorithm 2.

The beginning of the second stage is similar to Stage 1, but with a difference in that the generated images  $img$  are used to add or subtract from  $I$ , which leads to a new set of images, denoted as  $I'$ , as depicted in Line 11 of the algorithm. Specifically, for the images in  $I$  having different labels from the label  $c$ ,  $img$  will be added to them, whereas for the image having the same label,  $img$  will be subtracted from it. Then, we design the loss function to train  $Gen$ , the corresponding equation is demonstrated in Lines 13–16 of Algorithm 2.

---

**Algorithm 2:** Trigger Filtering

---

**Input:** i)  $G_{old}$ , old global model; ii)  $G_{agg}$ , new global model; iii)  $E$ , training rounds; iv)  $C$ , category number; v)  $\gamma, \lambda$ , balance coefficient; vi)  $I_{Gen}$ , set of generated images from Stage 1;

**Output:**  $T_{Gen}$ , set of trigger images;

```

1  $D1 \leftarrow G_{old}$ 
2  $D2 \leftarrow G_{agg}$ 
3  $z \leftarrow noise$ 
4  $Gen \leftarrow random$ 
5  $label \leftarrow \{0, 1, \dots, C - 1\}$ 
6 for  $epoch=0$  to  $E$  do
7    $Imgs \leftarrow Gen(z, label)$ 
8    $Loss \leftarrow 0$ 
9   for  $i=0$  to  $C$  do
10     $img \leftarrow Imgs(i)$ 
11     $I' \leftarrow I \pm img$ 
12     $Loss_{std} \leftarrow Mean(std(D1(I')))$ 
13     $Loss_{max} \leftarrow Mean(1 - D2(I'_{k \neq c}, c))$ 
14     $Loss_{min} \leftarrow D2(I'_c, c)$ 
15     $Loss \leftarrow \gamma \times Loss_{std} + \lambda \times Loss_{max} + (1 - \gamma - \lambda) \times Loss_{min} + Loss$ 
16  end
17  Update  $Gen$  by  $Loss$ 
18 end
19  $T \leftarrow Gen(z, label)$ 

```

---

Same as the loss function in Stage 1, there are also two hyperparameters, namely  $\gamma$  and  $\lambda$ , that are employed to balance the terms in the loss function. Similar to Stage 1, the first term of the loss function,  $Loss_{std}$ , presented in Line 12 of Algorithm 2, is aimed at minimizing the standard deviation

of  $D_1$  across all categories. This objective is intended to confine the scope of the generated image to the difference between  $G_{old}$  and  $G_{agg}$ . The second term of the loss function,  $Loss_{max}$ , as presented in Line 13, aims to maximize the probability of  $D_2$  classifying the generated image as the current class  $c$ . This objective suggests that adding the generated images to the original images would significantly increase the probability of them being classified as  $c$ , even if their original classifications were different. Finally, the third term of the loss function,  $Loss_{min}$ , presented in Line 14 of Algorithm 2, aims to minimize the probability of  $D_2$  classifying the generated image as  $c$ . This objective implies that subtracting the generated images from the original images should reduce the probability of them being classified as  $c$ . Overall, these three terms in the loss function work together to train the generation network  $Gen$ . By optimizing the loss function, the trained  $Gen$  can generate images that can easily perturb the image classification, which are identified to be the precise knowledge of triggers in  $I$ . Finally, we save the generated images for all categories, obtaining the trigger set  $T$  in Line 20 of Algorithm 2.

*E. Model Filtering*

In the third stage, we examine the models participating in the aggregation process using the backdoor triggers generated in the second stage ( $T$ ). The images in  $T$  exhibit certain distinguishing characteristics. Specifically, when the category of the trigger image is attacked, the poisoned model is able to classify the image into the category with a high degree of certainty, while the clean model may exhibit ambiguity in its classification. On the other hand, all models may exhibit ambiguity in classifying the images in  $T$  whose categories are not attacked. By leveraging these characteristics, we can identify the poisoned models. Therefore, we design the algorithm as shown in Algorithm 3.

---

**Algorithm 3:** Model Filtering

---

**Input:** i)  $N$ , number of participating clients; ii)  $M = \{M_0, M_1, \dots, M_{N-1}\}$ , set of the updated local models; iii)  $T$ , set of trigger images;

**Output:**  $G_{new}$ , new benign global model;

```

1 for  $i=0$  to  $N$  do
2   for  $c=0$  to  $C$  do
3      $Out \leftarrow M_i(T_c)$ 
4     if  $Argmax(Out) = c$  and  $Out(c) > \rho$  then
5       Remove  $M_i$  from  $M$ 
6   end
7 end
8  $G_{new} \leftarrow Aggregate(M')$ 

```

---

For each model in the set of the updated local models  $M$ , we send the trigger image in  $T$  into the model and compare the output classification with the category of the trigger, which shown in Line 3 in Algorithm 3. In Lines 4 and 5, we perform the check on the  $out$ . If the output classification is the

same as the trigger category and the classification confidence degree exceeds the threshold standard  $\rho$ , we consider the model to be particularly sensitive to the trigger image, which means the model is poisoned. Such models are excluded from participation in the subsequent aggregation process. In the end of the algorithm, we obtain a benign set of models, which we aggregate to obtain a new global model  $G_{new}$ , and the FL process moves to the next round.

## V. EXPERIMENTS

### A. Experiments Setup

To evaluate the effectiveness of our approach, we implemented the framework of our approach on top of Pytorch (version 1.13.0). All the experiments were conducted on a workstation with Ubuntu operating system, Intel i9-10900K CPU, 32GB memory, and NVIDIA GeForce GTX3080 GPU. We deployed our experiments on the classic FL architecture FedAvg [1]. We assume there are 100 clients involved in the FL and in each FL round, 10% of the clients were randomly selected for local training.

**Dataset settings** Our experimental evaluation was performed on four datasets, namely MNIST [31], CIFAR-10, CIFAR-100 [32], and GTSRB [33]. For MNIST, the local training round was set to one epoch with a learning rate of 0.1, while for the other datasets, each client trained for two epochs with a learning rate of 0.01. However, adversarial clients were allowed to set different training hyperparameters from benign clients. For instance, the adversarial clients trained for 10 epochs locally with a learning rate of 0.05 on MNIST. More detailed parameter settings, introduction of datasets and model structures can be found in the supplementary material A.

**Data heterogeneity settings** To evaluate the performance of our approach within both IID and non-IID scenarios, we adopted the Dirichlet distribution [34] denoted by coefficient  $\alpha$  to control the heterogeneity settings, where a smaller indicates a higher data heterogeneity of clients. By default, we set  $\alpha$  to 0.5 and used this value for the data distribution in the following experiments.

**Baseline settings** We compared our approach with seven state-of-the-art (SOTA) baseline methods, i.e., Krum [20], MKrum [20], COMED [22], RLR [30], Trimmed Mean [21], DP [23], FLAME [35]. Specifically, Krum, MKrum, COMED, RLR and Trimmed Mean are similarity-based methods, and DP is the representation of Differential Privacy (DP)-based methods, FLAME is an improved version of DP. More detailed introduction and settings can be found in the supplementary material D.

**Attack settings** We adopted the multiple basic attacks as our attack setting, wherein the attacker controls a subset of the total clients as the adversarial clients. The variable  $\eta$  represents the proportion of adversarial clients among all the clients. Whenever the server selects adversarial clients, these clients initiate the attacks. By default,  $\eta$  was set to 0.1.

### B. Performance Comparison

We compared our defense approach with seven state-of-the-art baselines on four well-known datasets (i.e., MNIST, CIFAR-10, CIFAR-100, and GTSRB) with both IID and three non-IID scenarios with  $\alpha = 0.1, 0.5$ , and  $1.0$ , respectively.

**Effectiveness on Different Datasets** Table I presents the Main task Accuracy (MA) and Attack Success Rate (ASR) of our approach and seven baselines on MNIST, CIFAR-10, CIFAR-100, and GTSRB datasets with  $\alpha = 0.5$ . From Table I, we can observe that our approach can achieve both the lowest ASR and best MA on MNIST and CIFAR-10 datasets. On CIFAR-100 dataset, our approach achieves the best MA and the second lowest ASR. Our ASR is only higher than that of Krum by 0.1%, but our MA is significantly higher than that of Krum by 8.68%. On the GTSRB dataset, our approach stands out with the lowest ASR among all the baselines. However, our MA falls slightly below the highest MA achieved by Trimmed Mean, with a difference of 0.24%. When considering the overall performance, it is worth noting that MKrum, RLR, and Trimmed Mean may have slightly higher MAs. Nonetheless, these methods exhibit significantly poorer ASR results, with values exceeding 91%, whereas our approach maintains an impressive ASR of only 0.14%. Moreover, we can observe that the majority of the baselines can achieve a good performance on MNIST, but on complex datasets, i.e., CIFAR-10, CIFAR-100, and GTSRB, all the baselines exhibit catastrophic performance. Compared with all the baselines, our approach can achieve a competitive MA while ensuring superior ASR performance on all the datasets.

**Impact of the Degree of Data Heterogeneity** Table II demonstrates the MA and ASR of our approach and seven baselines on CIFAR-10 dataset with IID and three non-IID scenarios with  $\alpha = 0.1, 0.5$ , and  $1.0$ , respectively. We can observe that our method can achieve similar performance to the no-attack case on IID and all the non-IID scenarios. In contrast, the majority of baselines only performed well in the IID scenarios. Although Krum achieved well ASR in all the non-IID scenarios, it causes a catastrophic drop in MA (i.e., 8.67%, 14.86%, and 35.09% with  $\alpha = 1.0, 0.5$ , and  $0.1$ , respectively). This is because the Krum method selects only one client in each epoch of aggregation, thereby effectively excluding poisoned models from the training process. However, when  $\alpha = 0.1$ , this defense method faces difficulties in achieving normal model convergence, resulting in a low MA. Since our method uses the natural characteristics of the backdoor trigger, which will not be affected by data heterogeneity, our method still maintains high performance in non-IID scenarios. Note that in the non-IID scenario, due to the decline in the inference ability of the model, the probability of the model misclassifying the poison image as the target image increases, which also can be observed in the case of no-attack. Therefore, the ASR of our method in the non-IID scenario has increased.

**Impact of the Number of Adversarial Clients** To explore the effectiveness of our approach and all the baselines to defend against multi-party coordinated attacks, we conduct

TABLE I  
EFFECTIVENESS OF OUR APPROACH IN COMPARISON TO SOTA DEFENSES AGAINST MULTIPLE ATTACKS ON FOUR DATASETS (MNIST, CIFAR-10, CIFAR-100, AND GTSRB) WITH  $\alpha = 0.5$ .

Defenses	MNIST		CIFAR-10		CIAFR-100		GTSRB	
	MA%	ASR%	MA%	ASR%	MA%	ASR%	MA%	ASR%
No Attack	98.38	0.22	85.52	2.51	54.31	0.50	95.63	0.20
No Defense	98.46	99.83	84.92	92.80	56.36	99.52	95.51	99.60
Krum [20]	93.05	1.23	70.66	7.22	46.27	<b>0.64</b>	94.30	0.22
MKrum [20]	98.24	0.32	84.17	78.07	53.35	94.65	95.69	97.28
COMED [22]	98.14	0.62	84.08	61.30	51.81	99.43	95.46	91.59
RLR [30]	93.85	1.84	76.93	8.30	26.64	42.25	94.13	34.26
Trimmed Mean [21]	98.19	0.69	84.59	64.54	52.04	99.47	<b>95.70</b>	91.59
DP [23]	90.61	85.66	71.23	84.21	41.56	89.70	90.44	88.80
FLAME [35]	98.16	0.37	81.85	93.78	51.52	98.24	94.76	66.78
Ours	<b>98.55</b>	<b>0.31</b>	<b>85.46</b>	<b>2.48</b>	<b>54.95</b>	0.65	95.45	<b>0.14</b>

TABLE II  
EFFECTIVENESS OF OUR APPROACH IN COMPARISON TO SOTA DEFENSES AGAINST MULTIPLE ATTACKS ON CIFAR-10, WITH ONE IID AND THREE NON-IID SCENARIOS ( $\alpha = 1, 0.5, 0.1$ ).

Defense	IID		$\alpha = 1$		$\alpha = 0.5$		$\alpha = 0.1$	
	MA%	ASR%	MA%	ASR%	M%	ASR%	MA%	ASR%
No Attack	86.53	2.31	86.59	2.06	85.52	2.51	74.17	6.50
No Defense	84.33	91.73	85.22	88.92	84.92	92.80	77.12	97.04
Krum [20]	84.78	2.76	77.83	3.26	70.66	7.22	39.08	<b>3.74</b>
MKrum [20]	86.10	21.59	86.09	72.77	84.17	78.07	68.20	97.85
COMED [22]	86.28	10.76	85.95	30.22	84.08	61.30	64.37	98.59
RLR [30]	78.84	3.89	80.58	<b>0.80</b>	76.93	8.30	68.66	89.36
Trimmed Mean [21]	86.20	14.32	86.10	30.50	84.59	64.54	66.81	97.08
DP [23]	71.13	84.48	71.95	84.05	71.23	84.21	56.73	89.35
FLAME [35]	85.56	10.85	84.24	87.17	81.85	93.78	66.89	98.86
Ours	<b>86.66</b>	<b>2.33</b>	<b>86.70</b>	2.27	<b>85.46</b>	<b>2.48</b>	<b>72.63</b>	7.42

TABLE III  
EFFECTIVENESS OF OUR APPROACH IN COMPARISON TO SOTA DEFENSES AGAINST MULTIPLE ATTACKS WITH DIFFERENT PROPORTIONS OF ADVERSARIAL CLIENTS ( $\eta = 0.1, 0.2, 0.5, 0.8$ ) ON MNIST DATASETS WITH  $\alpha = 0.5$ .

Defenses	$\eta = 0.1$		$\eta = 0.2$		$\eta = 0.5$		$\eta = 0.8$	
	MA%	ASR%	MA%	ASR%	MA%	ASR%	MA%	ASR%
No Attack	98.38	0.22	98.38	0.22	98.38	0.22	98.38	0.22
No Defense	98.46	99.83	98.64	99.98	98.63	100.00	98.60	100.00
Krum [20]	93.05	1.23	94.11	0.75	88.02	95.38	97.09	99.84
MKrum [20]	98.24	0.32	98.22	86.36	98.25	99.97	98.41	100.00
COMED [22]	98.14	0.62	<b>98.32</b>	97.51	98.58	99.99	98.51	100.00
RLR [30]	93.85	1.84	98.29	99.33	97.80	99.31	98.10	100.00
Trimmed Mean [21]	98.19	0.69	98.31	99.55	<b>98.61</b>	100.00	<b>98.59</b>	100.00
DP [23]	90.61	85.66	90.23	84.21	86.56	95.70	84.44	99.80
FLAME [35]	98.16	0.37	98.16	2.33	98.45	100.00	98.44	100.00
Ours	<b>98.55</b>	<b>0.31</b>	<b>98.32</b>	<b>0.21</b>	94.96	<b>0.33</b>	93.82	<b>0.85</b>

experiments for different proportions of adversarial clients, i.e.,  $\eta = 0.1, 0.2, 0.5$ , and  $0.8$ , respectively. Table III shows all the MA and ASR of our approach and all the baselines on MNIST dataset for different numbers of adversarial clients with  $\alpha = 0.5$ . From Table III, we can observe that our approach can achieve significant defense performance with all the settings of  $\eta$ . For the baselines, only FLAME and Krum can effectively defend attacks with  $\eta = 0.2$ . When  $\eta = 0.5$  or  $0.8$ , none of the baselines can efficiently defend against attacks. Due to exploiting the characteristics of backdoor triggers instead of model similarity, our approach can still

achieve a low ASR by  $0.85\%$ . However, we can observe that MA of our approach is dropped by  $4.56\%$ , which is attributed to the limited number of benign clients contributing to the model aggregation. Nonetheless, our approach still provides effective protection against backdoor attacks.

### C. Ablation Studies

As previously described, the second stage of our approach plays a critical role in distinguishing between normal categories knowledge and backdoor trigger knowledge. To demonstrate the importance of this stage, we conducted the ablation



TABLE IV  
EFFECTIVENESS OF THE ABLATION OF OUR APPROACH AGAINST MULTIPLE ATTACKS ON GTSRB, WITH ONE IID AND THREE NON-IID SCENARIOS ( $\alpha = 1, 0.5, 0.1$ ).

Defenses	IID		$\alpha = 1$		$\alpha = 0.5$		$\alpha = 0.1$	
	MA%	ASR%	MA%	ASR%	MA%	ASR%	MA%	ASR%
No Attack	96.52	0.10	95.63	0.12	95.63	0.20	96.36	0.06
No Defense	96.59	99.76	95.89	99.75	95.51	99.60	96.24	98.79
Full Approach	96.36	0.11	95.57	0.14	95.45	0.14	96.04	0.48
Without Stage 2	85.51	0.13	71.2	1.32	94.68	41.61	93.31	89.69

experiment where we fed the set of images  $I_{Gen}$  generated in Stage 1 directly into Stage 3, while keeping other settings unchanged. The results of the experiment are presented in Table IV. The table reveals that the ablated approach remains effective in the IID scenario, though there is a reduction in MA, which can be attributed to the wrong exclusion of some benign models, thereby impeding the convergence rate. In contrast, the efficacy of the ablated approach gradually declines with a decrease in the  $\alpha$  value of non-IID scenario. Notably, when  $\alpha$  is equal to 0.5, MA of the ablated approach increases once again. This can be attributed to the fact that in situations where the data distribution is extreme, the ablated approach struggles to distinguish between normal category knowledge and backdoor trigger knowledge. As a result, there are several misjudgments of the poisoned models, and these models will participate in the aggregation of global model, leading to the convergence rate of the global model become normal. when  $\alpha$  equals 0.1, the ablated approach is completely ineffective. These ablation experiments highlight the significance of Stage 2 in ensuring the effectiveness of our approach under extreme data distribution scenarios.

## VI. CONCLUSION

In this work, we proposed a novel backdoor defense approach on federated learning using data-free trigger generation, which is based on two characteristics of the backdoor triggers, i.e., easy to be learned and strong perturbation to change the classification. By leveraging the differences between the old and new global models, our approach generates images for the new knowledge of each category. Then, our approach filters from these images to get the trigger images, which aims to make other images be misclassified when overlapping them. In this way, our approach can precisely generate triggers without any raw data. By using these generated triggers, the server can effectively detect and eliminate the poisoned models, while minimizing the risk of false exclusions. The experimental results on four well-known datasets demonstrate the effectiveness and pervasiveness of our approach.

## REFERENCES

- [1] Brendan McMahan, Eider Moore, Daniel Ramage, Seth Hampson, and Blaise Agüera y Arcas. Communication-efficient learning of deep networks from decentralized data. In *Artificial intelligence and statistics*, pages 1273–1282. PMLR, 2017.
- [2] Tian Li, Anit Kumar Sahu, Ameet Talwalkar, and Virginia Smith. Federated learning: Challenges, methods, and future directions. *IEEE signal processing magazine*, 37(3):50–60, 2020.
- [3] Jakub Konečný, Brendan McMahan, and Daniel Ramage. Federated optimization: Distributed optimization beyond the datacenter. *arXiv preprint arXiv:1511.03575*, 2015.
- [4] Yue Zhao, Meng Li, Liangzhen Lai, Naveen Suda, Damon Civin, and Vikas Chandra. Federated learning with non-iid data. *arXiv preprint arXiv:1806.00582*, 2018.
- [5] Quande Liu, Cheng Chen, Jing Qin, Qi Dou, and Pheng-Ann Heng. Feddgc: Federated domain generalization on medical image segmentation via episodic learning in continuous frequency space. In *Proceedings of the IEEE/CVF Conference on Computer Vision and Pattern Recognition*, pages 1013–1023, 2021.
- [6] Hongyi Zhang, Jan Bosch, and Helena Holmström Olsson. End-to-end federated learning for autonomous driving vehicles. In *Proceedings of International Joint Conference on Neural Networks (IJCNN)*, pages 1–8, 2021.
- [7] Xinqian Zhang, Ming Hu, Jun Xia, Tongquan Wei, Mingsong Chen, and Shiyan Hu. Efficient federated learning for cloud-based aiot applications. *IEEE Transactions on Computer-Aided Design of Integrated Circuits and Systems*, 40(11):2211–2223, 2020.
- [8] Ming Hu, Zeke Xia, Zhihao Yue, Jun Xia, Yihao Huang, Yang Liu, and Mingsong Chen. Gitfl: Adaptive asynchronous federated learning using version control. *arXiv preprint arXiv:2211.12049*, 2022.
- [9] Eugene Bagdasaryan, Andreas Veit, Yiqing Hua, Deborah Estrin, and Vitaly Shmatikov. How to backdoor federated learning. In *International Conference on Artificial Intelligence and Statistics*, pages 2938–2948. PMLR, 2020.
- [10] Hongyi Wang, Kartik Sreenivasan, Shashank Rajput, Harit Vishwakarma, Saurabh Agarwal, Jy-yong Sohn, Kangwook Lee, and Dimitris Papailiopoulos. Attack of the tails: Yes, you really can backdoor federated learning. *Advances in Neural Information Processing Systems*, 33:16070–16084, 2020.
- [11] Chulin Xie, Keli Huang, Pin-Yu Chen, and Bo Li. Dba: Distributed backdoor attacks against federated learning. In *International conference on learning representations*, 2020.
- [12] Tianyu Gu, Brendan Dolan-Gavitt, and Siddharth Garg. Badnets: Identifying vulnerabilities in the machine learning model supply chain. *arXiv preprint arXiv:1708.06733*, 2017.
- [13] Yingqi Liu, Shiqing Ma, Yousra Aafer, Wen-Chuan Lee, Juan Zhai, Weihang Wang, and Xiangyu Zhang. Trojaning attack on neural networks. In *25th Annual Network And Distributed System Security Symposium (NDSS 2018)*. Internet Soc, 2018.
- [14] Anh Nguyen and Anh Tran. Wanet-imperceptible warping-based backdoor attack. *arXiv preprint arXiv:2102.10369*, 2021.
- [15] Kang Liu, Brendan Dolan-Gavitt, and Siddharth Garg. Fine-pruning: Defending against backdooring attacks on deep neural networks. In *Research in Attacks, Intrusions, and Defenses: 21st International Symposium, RAID 2018, Heraklion, Crete, Greece, September 10-12, 2018, Proceedings 21*, pages 273–294. Springer, 2018.
- [16] Yige Li, Xixiang Lyu, Nodens Koren, Lingjuan Lyu, Bo Li, and Xingjun Ma. Neural attention distillation: Erasing backdoor triggers from deep neural networks. *arXiv preprint arXiv:2101.05930*, 2021.
- [17] Bolun Wang, Yuanshun Yao, Shawn Shan, Huiying Li, Bimal Viswanath, Haitao Zheng, and Ben Y Zhao. Neural cleanse: Identifying and mitigating backdoor attacks in neural networks. In *2019 IEEE Symposium on Security and Privacy (SP)*, pages 707–723. IEEE, 2019.

- [18] Yige Li, Xixiang Lyu, Nodens Koren, Lingjuan Lyu, Bo Li, and Xingjun Ma. Anti-backdoor learning: Training clean models on poisoned data. *Advances in Neural Information Processing Systems*, 34:14900–14912, 2021.
- [19] Yiming Li, Yong Jiang, Zhifeng Li, and Shu-Tao Xia. Backdoor learning: A survey. *IEEE Transactions on Neural Networks and Learning Systems*, 2022.
- [20] Peva Blanchard, El Mahdi El Mhamdi, Rachid Guerraoui, and Julien Stainer. Machine learning with adversaries: Byzantine tolerant gradient descent. *Advances in neural information processing systems*, 30, 2017.
- [21] Cong Xie, Oluwasanmi Koyejo, and Indranil Gupta. Generalized byzantine-tolerant sgd. *arXiv preprint arXiv:1802.10116*, 2018.
- [22] Dong Yin, Yudong Chen, Ramchandran Kannan, and Peter Bartlett. Byzantine-robust distributed learning: Towards optimal statistical rates. In *International Conference on Machine Learning*, pages 5650–5659. PMLR, 2018.
- [23] Ziteng Sun, Peter Kairouz, Ananda Theertha Suresh, and H Brendan McMahan. Can you really backdoor federated learning? *arXiv preprint arXiv:1911.07963*, 2019.
- [24] Cynthia Dwork, Aaron Roth, et al. The algorithmic foundations of differential privacy. *Foundations and Trends® in Theoretical Computer Science*, 9(3–4):211–407, 2014.
- [25] Dongxian Wu and Yisen Wang. Adversarial neuron pruning purifies backdoored deep models. *Advances in Neural Information Processing Systems*, 34:16913–16925, 2021.
- [26] Hossein Souri, Liam Fowl, Rama Chellappa, Micah Goldblum, and Tom Goldstein. Sleeper agent: Scalable hidden trigger backdoors for neural networks trained from scratch. *Advances in Neural Information Processing Systems*, 35:19165–19178, 2022.
- [27] Lingjuan Lyu, Han Yu, Xingjun Ma, Chen Chen, Lichao Sun, Jun Zhao, Qiang Yang, and S Yu Philip. Privacy and robustness in federated learning: Attacks and defenses. *IEEE transactions on neural networks and learning systems*, 2022.
- [28] Mehdi Mirza and Simon Osindero. Conditional generative adversarial nets. *arXiv preprint arXiv:1411.1784*, 2014.
- [29] Zhengming Zhang, Ashwinee Panda, Linyue Song, Yaoqing Yang, Michael Mahoney, Prateek Mittal, Ramchandran Kannan, and Joseph Gonzalez. Neurotoxin: Durable backdoors in federated learning. In *International Conference on Machine Learning*, pages 26429–26446. PMLR, 2022.
- [30] Mustafa Safa Ozdayi, Murat Kantarcioglu, and Yulia R Gel. Defending against backdoors in federated learning with robust learning rate. In *Proceedings of the AAAI Conference on Artificial Intelligence*, volume 35, pages 9268–9276, 2021.
- [31] Yann LeCun, Lawrence D Jackel, Léon Bottou, Corinna Cortes, John S Denker, Harris Drucker, Isabelle Guyon, Urs A Muller, Eduard Sackinger, Patrice Simard, et al. Learning algorithms for classification: A comparison on handwritten digit recognition. *Neural networks: the statistical mechanics perspective*, 261(276):2, 1995.
- [32] Alex Krizhevsky, Geoffrey Hinton, et al. Learning multiple layers of features from tiny images. 2009.
- [33] Johannes Stallkamp, Marc Schlipsing, Jan Salmen, and Christian Igel. Man vs. computer: Benchmarking machine learning algorithms for traffic sign recognition. *Neural networks*, 32:323–332, 2012.
- [34] Tzu-Ming Harry Hsu, Hang Qi, and Matthew Brown. Measuring the effects of non-identical data distribution for federated visual classification. *arXiv preprint arXiv:1909.06335*, 2019.
- [35] Thien Duc Nguyen, Phillip Rieger, Roberta De Viti, Huili Chen, Björn B Brandenburg, Hossein Yalame, Helen Möllering, Hossein Fereidooni, Samuel Marchal, Markus Miettinen, et al. {FLAME}: Taming backdoors in federated learning. In *31st USENIX Security Symposium (USENIX Security 22)*, pages 1415–1432, 2022.

## APPENDIX

### A. Datasets and Networks

The datasets and DNN models used in our experiments are summarized in Table V.

### B. FL Details

Table VI presents the detailed setup of federated learning in our experiments.

TABLE V  
DETAILED INFORMATION OF THE DATASETS AND CLASSIFIERS USED IN OUR EXPERIMENTS.

Dataset	Labels	Input Size	Total Training Images	Classifier
MNIST	10	$28 \times 28 \times 1$	60000	CNN
CIFAR-10	10	$32 \times 32 \times 3$	50000	ResNet-8
CIFAR-100	100	$32 \times 32 \times 3$	50000	ResNet-18
GTSRB	43	$32 \times 32 \times 3$	39252	ResNet-8

### C. Setup of Adversarial Clients

Table VII presents of the detailed local training setup for the adversarial clients.

### D. Baseline Settings Details

**Krum** [20] is a Byzantine-robust aggregation rule which originally designed to mitigate Byzantine attacks. Krum is based on the similarity of gradients or parameters of models provided by the selected clients at each round of FL. During the aggregation process, Krum chooses the local model that is most similar to the others by Euclidean distance and selects it as the global model.

**MKrum** [20] is a variant of Krum that aims to address the issue of slow convergence. MKrum improves upon Krum by repeating the Krum algorithm  $m$  times, each time MKrum will remove the selected model from the set of uploaded models. Finally, the  $m$  selected local models will be aggregated to form the new global model. In our experiments,  $m$  was set as 5.

**COMED** [22] changes the aggregation strategy, which selects the median rather than the average for each parameter of models when aggregating the global model.

**RLR** [30] adjusts the aggregation server’s learning rate, per dimension and per round, based on the sign information of clients’ updates in order to make the global model update towards a particular direction. In this way, the direction of backdoor as a minority will be excluded. RLR sets the learning rate according to the equation 1. In our experiments,  $\theta$  was set as 4.

$$\eta_{\theta,i} = \begin{cases} \eta & |\sum_{k \in S_t} \text{sgn}(\delta_{t,i}^k)| \geq \theta \\ -\eta & \text{otherwise} \end{cases} \quad (1)$$

**Trimmed Mean** [21] sorts the uploaded models according to each parameter. Then Trimmed Mean removes the largest and smallest  $k$  clients and calculates the average of the remaining clients for each parameter to update the global model. In our experiments,  $k$  was set as 3.

**DP** [23] eliminates the influence of the backdoor by adding Gaussian noise to the uploaded models. In our experiments, the  $\sigma$  of the Gaussian noise was set as 0.015.

**FLAME** [35] is a defense framework that estimates the sufficient amount of noise to be injected to ensure the elimination of backdoor and uses a model clustering and weight clipping approach to minimize the required amount of noise. FLAME uses HDBSCAN to cluster the models. In our experiments, the distance of HDBSCAN was calculated using cosine similarity, min\_cluster\_size was set as the 6 and min\_samples was 1.

TABLE VI  
DETAILED SETUP OF FEDERATED LEARNING FOR EACH DATASET.

Dataset	MNIST	CIFAR-10	CIFAR-100	GTSRB
Global Epoch	100	2000	2000	1000
Local Epoch	1	2	2	2
Total Clients	100	100	100	100
Selected Clients	10	10	10	10
Learning Rate	0.1	0.01	0.01	0.01
momentum	0.9	0.9	0.9	0.9
decay	0.001	0.0005	0.0005	0.0005
Data Augmentation	None	Random crop (32, 4) RandomHorizontalFlip	Random crop (32, 4) RandomHorizontalFlip	Random crop(32, 4)

TABLE VII  
DETAILED SETUP OF LOCAL TRAINING FOR THE ADVERSARIAL CLIENTS FOR EACH DATASET.

Dataset	MNIST	CIFAR-10	CIFAR-100	GTSRB
Local Epoch	10	6	6	6
Learning Rate	0.05	0.001	0.001	0.001
Poison Rate	0.5	0.5	0.5	0.5
Target Label	2	bird	otter	Speed limit 50

#### E. Effectiveness on Different Datasets and Degrees of Data Heterogeneity

Table VIII illustrates our approach compared to state-of-the-art (SOTA) defense methods on four datasets: MNIST, CIFAR-10, CIFAR-100, and GTSRB. We evaluate the performance of our approach with one IID and three non-IID ( $\alpha = 1, 0.5, 0.1$ ) data distributions scenarios. The results demonstrate the efficacy and robustness of our approach across diverse datasets and data distributions.

#### F. Effectiveness against Different Attacks

Table IX presents that our approach against SOTA attacks on CIFAR-10 and GTSRB dataset with the non-IID scenario ( $\alpha = 0.5$ ). For the multiple attack, we randomly chose 10 clients as the adversarial clients, whenever the adversarial clients selected by the server of FL, the clients would inject the backdoor into their local models to participate in the aggregation. For the single attack, we randomly chose only one client as the adversarial, the client wouldn't make attack until the global model was closed to convergence, namely that the current global epoch was in the last 10% of the total global epoch. DBA [11] makes use of the distributed characteristics of FL and divides the trigger pattern into multiple parts to realize the distributed backdoor attack, and Neurotoxin [29] preferentially trains those model parameters with few changes when the backdoor is injected, both of which improve the stealth and persistence of backdoor attacks. Experimental results show that our approach can well protect the global model against SOTA backdoor attacks.

#### G. Impact of Number of Adversarial Clients in each Round

To further explore the effectiveness of our approach against numerous adversarial clients, we designed the experiments, there are fixed number of adversarial clients in the selected clients in each round. The results of the experiments are shown

in Table X. The experimental results show that the similarity-based methods will lose the effect when the benign models are no longer the majority. Specifically, when the number of adversarial clients in each round of FL was 3, Krum and MKrum still have defensive effects. While the number was 5, only Krum remains defensive. And when adversarial clients are the majority, namely the number was 8, none of the SOTA methods can efficiently defend against attacks. However, we can observe that our approach always effectively defends against attacks with different numbers of adversarial clients in each round of FL.

#### H. Impact of Hyperparameter $\rho$

In order to explore the impact of hyperparameter  $\rho$  on the effect of our approach, we designed the experiments, and the results are shown in the Table XI. The experiments show that when the value of  $\rho$  is too small, benign models will be excluded unexpectedly, resulting in the decline of MA; when the value of  $\rho$  is too large, some poisoned models may be missed, resulting in defense failure. This phenomenon is especially obvious in the case of extreme data distribution. Finally, we decide to set the value of  $\rho$  as 0.5.

#### I. Choice of Training Rounds and Extra Time Overhead

We determined the training rounds of CGANs in our approach from two aspects: the effectiveness of the approach and the size of the extra time overhead. We designed the experiments that we gradually increased the training rounds of CGANs, observed the effectiveness of our approach and the comparison of the extra time overhead with other SOTA defense methods, and determined the training rounds we finally chose. The extra time overheads of the SOTA defense methods are shown in Table XII, and Table XIII shows the results of experiments. It can be found from the results that when the number of training rounds is 10, our approach already has a

TABLE VIII  
EFFECTIVENESS OF OUR APPROACH IN COMPARISON TO SOTA DEFENSES AGAINST MULTIPLE ATTACKS( $\eta = 0.1$ ) ON FOUR DATASETS WITH ONE IID AND THREE NON-IID SCENARIOS.

Distribution	Defense	MNIST		CIFAR-10		CIFAR-100		GTSRB	
		MA%	ASR%	MA%	ASR%	MA%	ASR%	MA%	ASR%
IID	No Attack	98.70	0.12	86.53	2.31	52.28	0.60	96.52	0.10
	No Defense	98.77	99.84	84.33	91.73	54.55	99.71	96.59	99.76
	Krum	97.59	0.34	84.78	2.76	50.19	<b>0.70</b>	95.74	0.17
	mKrum	98.53	0.21	86.10	21.59	52.62	3.11	96.11	56.92
	COMED	98.50	0.43	86.28	10.76	53.80	99.39	96.26	91.29
	RLR	98.40	61.94	78.84	13.89	35.78	23.44	94.88	0.67
	Trimmed Mean	98.00	1.13	86.20	14.32	<b>53.88</b>	99.40	96.21	93.92
	DP	90.32	84.25	71.13	84.48	38.65	89.86	91.95	88.73
	FLAME	98.45	0.32	85.56	10.85	51.81	1.49	95.82	33.82
	Ours	<b>98.60</b>	<b>0.20</b>	<b>86.66</b>	<b>2.33</b>	52.22	<b>0.70</b>	<b>96.36</b>	<b>0.11</b>
$\alpha = 1$	No Attack	98.27	0.24	86.59	2.06	55.08	0.70	95.63	0.12
	No Defense	98.75	99.57	85.22	88.92	56.49	99.58	95.89	99.75
	Krum	95.84	0.49	77.83	3.26	50.31	<b>0.4</b>	95.23	0.29
	mKrum	98.11	0.34	86.09	72.77	53.27	82.47	95.27	91.94
	COMED	98.48	0.44	85.95	30.22	54.30	99.37	<b>95.74</b>	90.46
	RLR	98.29	11.02	80.58	<b>0.80</b>	34.56	28.68	94.31	49.52
	Trimmed Mean	98.50	0.72	86.10	30.50	54.49	99.50	91.76	94.50
	DP	91.61	86.87	71.95	84.05	41.33	89.66	90.69	88.56
	FLAME	98.21	0.30	84.24	87.17	52.32	81.21	94.95	44.84
	Ours	<b>98.64</b>	<b>0.22</b>	<b>86.70</b>	2.27	<b>54.56</b>	0.59	95.57	<b>0.14</b>
$\alpha = 0.5$	No Attack	98.38	0.22	85.52	2.51	54.31	0.50	95.63	0.20
	No Defense	98.46	99.83	84.92	92.80	56.36	99.52	95.51	99.60
	Krum	93.05	1.23	70.66	7.22	46.27	<b>0.64</b>	94.30	0.22
	mKrum	98.24	0.32	84.17	78.07	53.35	94.65	95.69	97.28
	COMED	98.14	0.62	84.08	61.30	51.81	99.43	95.46	91.59
	RLR	93.85	1.84	76.93	8.30	26.64	42.25	94.13	34.26
	Trimmed Mean	98.19	0.69	84.59	64.54	52.04	99.47	<b>95.70</b>	91.59
	DP	90.61	85.66	71.23	84.21	41.56	89.75	90.44	88.80
	FLAME	98.16	0.37	81.85	93.78	51.52	98.24	94.76	66.78
	Ours	<b>98.55</b>	<b>0.31</b>	<b>85.46</b>	<b>2.48</b>	<b>54.95</b>	0.65	95.45	<b>0.14</b>
$\alpha = 0.1$	No Attack	97.65	0.32	74.17	6.50	50.97	0.58	96.36	0.06
	No Defense	97.53	99.75	77.12	97.04	53.24	99.41	96.24	98.79
	Krum	10.60	2.31	39.08	<b>3.74</b>	25.93	0.82	44.29	16.46
	mKrum	96.57	0.84	68.20	97.85	48.88	93.55	96.33	86.22
	COMED	95.11	0.71	64.37	98.59	36.51	99.63	93.32	92.09
	RLR	<b>97.32</b>	98.88	68.66	89.36	19.80	57.12	95.92	99.08
	Trimmed Mean	95.97	1.79	66.81	97.08	38.19	99.74	95.83	98.69
	DP	88.95	89.46	56.73	89.35	37.44	89.73	89.93	86.79
	FLAME	94.43	90.17	66.89	98.86	46.68	99.61	93.92	97.41
	Ours	97.23	<b>0.70</b>	<b>72.63</b>	7.42	<b>50.70</b>	<b>0.60</b>	<b>96.04</b>	<b>0.48</b>

satisfactory effect, but when the number of training rounds continues to increase, the effect cannot be greatly improved, instead leads to too much extra time overheads. Finally, according to the experiments, we chose 10 as the number of training rounds for our approach to train the CGANs.

### J. Effectiveness under Privacy Protection

In order to prevent privacy leakage and member inference attacks, clients in FL use Local Differential Privacy (LDP) to protect their local datasets. We designed experiments to verify the effectiveness of our approach when using privacy protection. The experiments are mainly divided into two situations: i) the adversarial clients do not use LDP to protect their datasets, and ii) the adversarial clients use LDP like the other benign clients. We use the symbol  $\varepsilon$  to represent the privacy budget, where the smaller value of  $\varepsilon$  indicates a higher degree of protection. We conducted experiments on MNIST dataset, with the non-IID scenario ( $\alpha = 0.5$ ). Table XIV shows the results of experiments. From the table, we can observe that

as the value of  $\varepsilon$  decreases, namely more noise will be added, MA of FL will decrease. When the adversarial clients use LDP, the ASR will be also slightly lower. And, in either case, our defense approach is still effective.

Figure 6 7 8 9 respectively illustrate our approach compared to SOTA defense methods on four datasets: MNIST, CIFAR-10, CIFAR-100, and GTSRB. We evaluate the performance of our approach with one IID and three non-IID ( $\alpha = 1, 0.5, 0.1$ ) data distributions scenarios. The figures demonstrate the efficacy and robustness of our approach across diverse datasets and data distributions.

TABLE IX  
EFFECTIVENESS OF OUR APPROACH AGAINST SOTA ATTACKS ON CIFAR-10 AND GTSRB DATASETS WITH THE NON-IID SCENARIO( $\alpha = 0.5$ ).

Attack	CIFAR-10				GTSRB			
	No Defense		Ours		No Defense		Ours	
	MA%	ASR%	MA%	ASR%	MA%	ASR%	MA%	ASR%
Multiple Attack	84.92	92.80	85.46	2.48	95.51	99.60	95.45	0.14
Single Attack	81.00	67.65	85.89	1.89	90.51	51.49	95.75	0.17
DBA(MA)	84.56	97.61	84.93	2.34	95.44	99.96	95.21	0.22
DBA(SA)	73.96	79.75	86.15	2.04	92.05	66.56	95.70	0.26
Neurotoxin(MA)	82.11	93.13	85.42	1.72	93.36	99.40	95.66	0.41
Neurotoxin(SA)	81.68	88.63	85.63	1.65	92.36	95.40	95.53	0.52

TABLE X  
EFFECTIVENESS OF OUR APPROACH IN COMPARISON TO SOTA DEFENSES AGAINST MULTIPLE ATTACKS WITH DIFFERENT NUMBERS OF ADVERSARIAL CLIENTS IN EACH ROUND ( $num = 1, 2, 3, 5, 8$ ) ON MNIST DATASET WITH THE NON-IID SCENARIO ( $\alpha = 0.5$ ).

Defenses	$num = 1$		$num = 2$		$num = 3$		$num = 5$		$num = 8$	
	MA%	ASR%	MA%	ASR%	MA%	ASR%	MA%	ASR%	MA%	ASR%
No Attack	98.38	0.22	98.38	0.22	98.38	0.22	98.38	0.22	98.38	0.22
No Defense	98.56	99.95	98.63	100.00	98.71	100.00	98.71	100.00	98.64	100.00
Krum	91.63	1.08	91.81	1.66	92.47	1.38	94.04	0.88	94.99	99.93
mKrum	97.89	0.31	97.88	<b>0.36</b>	97.97	0.41	98.24	100.00	98.19	100.00
COMED	98.07	0.54	95.15	6.37	98.28	98.58	98.51	100.00	98.50	100.00
RLR	97.47	3.60	96.42	82.06	98.32	97.62	98.41	99.62	98.32	100.00
Trimmed Mean	98.17	0.56	98.25	9.86	98.37	99.69	98.61	100.00	98.57	100.00
DP	96.38	87.95	<b>98.59</b>	99.90	<b>98.68</b>	99.96	<b>98.70</b>	100.00	98.69	100.00
FLAME	98.13	0.34	98.14	1.89	98.18	19.19	98.55	100.00	98.58	100.00
Ours	<b>98.56</b>	<b>0.30</b>	98.51	0.40	98.15	<b>0.35</b>	95.55	<b>0.45</b>	<b>94.55</b>	<b>0.75</b>

TABLE XI  
EFFECTIVENESS OF OUR APPROACH WITH DIFFERENT HYPERPARAMETER  $\rho$  ON CIFAR-10 WITH ONE IID AND THREE NON-IID SCENARIOS ( $\alpha = 1, 0.5, 0.1$ ).

$\rho$	IID		$\alpha = 1$		$\alpha = 0.5$		$\alpha = 0.1$	
	MA%	ASR%	MA%	ASR%	MA%	ASR%	MA%	ASR%
0.20	85.58	2.25	81.51	2.34	65.34	3.63	45.63	8.31
0.30	86.26	2.40	86.51	2.12	81.89	2.57	62.45	7.66
0.40	86.54	2.26	86.69	2.27	85.46	2.44	72.59	7.44
0.50	86.66	2.33	86.70	2.27	85.46	2.48	72.63	7.42
0.60	86.53	2.31	86.66	3.26	84.58	15.87	75.45	45.52
0.70	85.45	7.46	86.57	10.02	84.97	62.34	76.69	91.23

TABLE XII  
EXTRA TIME OVERHEADS OF THE SOTA DEFENSE METHODS ON CIFAR-100 DATASET. THE FIRST LINE REPRESENTS THE AVERAGE TIME OVERHEAD PER CLIENT DURING NORMAL TRAINING.

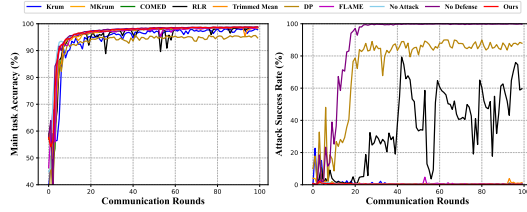
Defenses	Extra Overhead (s)
Normal Training	1.335
Krum	0.663
mKrum	1.426
COMED	0.059
RLR	0.063
Trimmed Mean	0.066
DP	0.055
FLAME	1.132

TABLE XIII  
EFFECTIVENESS AND EXTRA TIME OVERHEADS OF OUR APPROACH WITH DIFFERENT TRAINING ROUNDS ON CIFAR-100 DATASET WITH THE NON-IID SCENARIO ( $\alpha = 0.1$ )

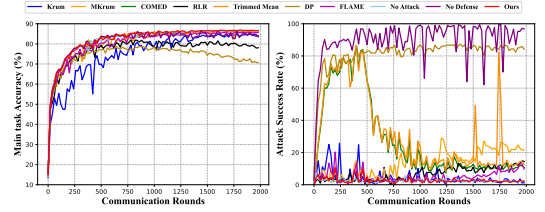
Training Rounds	2		5		10		15		20	
Effectiveness %	MA	ASR	MA	ASR	MA	ASR	MA	ASR	MA	ASR
	52.17	87.60	50.97	3.88	50.70	0.60	50.71	0.59	50.70	0.61
Extra Overhead (s)	0.872		2.126		3.852		6.033		7.213	

TABLE XIV  
EFFECTIVENESS OF OUR APPROACH UNDER PRIVACY PROTECTION ON MNIST DATASET WITH THE NON-IID SCENARIO ( $\alpha = 0.5$ ).

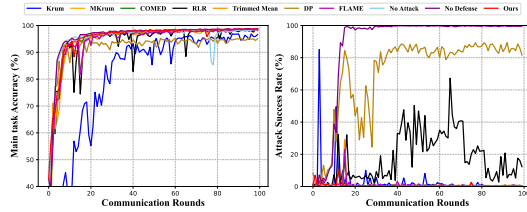
$\epsilon$	Adversarial Clients don't use LDP				Adversarial Clients use LDP			
	No Defense		Ours		No Defense		Ours	
	MA%	ASR%	MA%	ASR%	MA%	ASR%	MA%	ASR%
$+\infty$	98.46	99.83	98.55	0.31	98.47	99.83	98.47	0.31
30	91.43	99.77	91.23	0.33	91.23	99.88	91.23	0.37
20	91.19	99.69	90.62	0.28	90.45	99.63	90.45	0.32
10	87.02	99.89	85.56	0.42	85.76	96.24	85.76	0.33
5	57.66	99.94	51.23	0.98	57.62	91.66	57.62	1.06
1	19.22	99.91	18.96	1.23	15.43	85.47	15.43	1.35



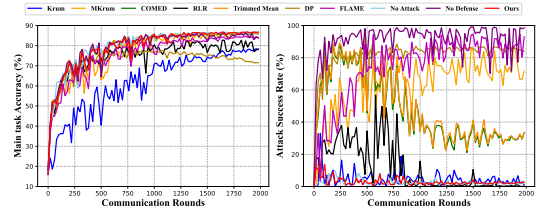
(a) IID



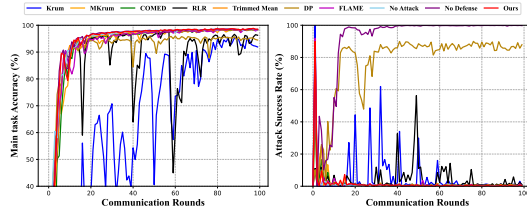
(a) IID



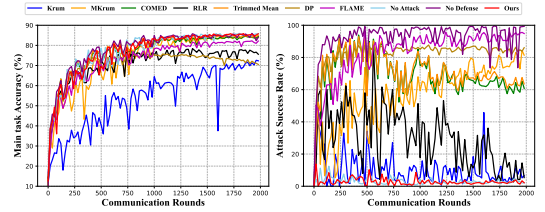
(b)  $\alpha = 1$



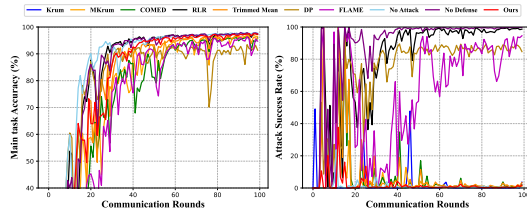
(b)  $\alpha = 1$



(c)  $\alpha = 0.5$

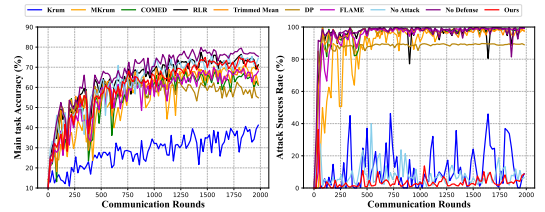


(c)  $\alpha = 0.5$



(d)  $\alpha = 0.1$

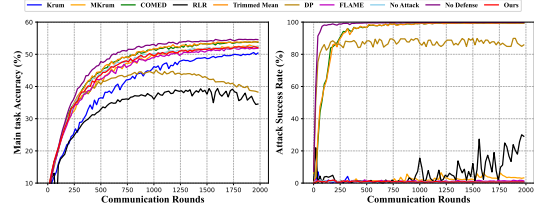
Fig. 6. MNIST



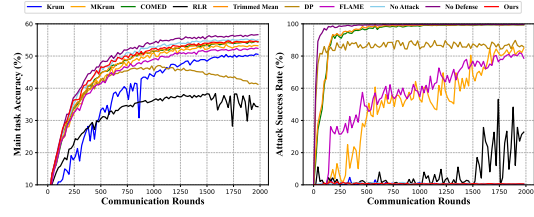
(d)  $\alpha = 0.1$

Fig. 7. CIFAR-10

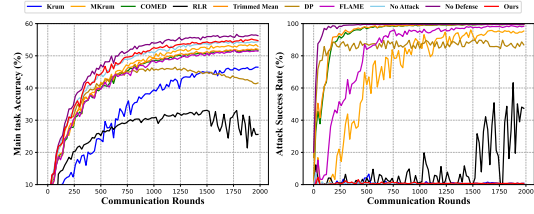




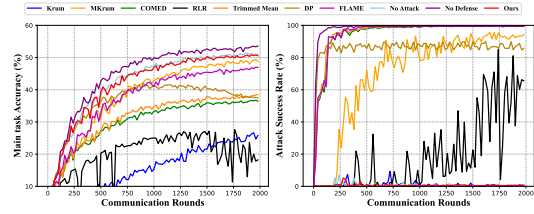
(a) IID



(b)  $\alpha = 1$

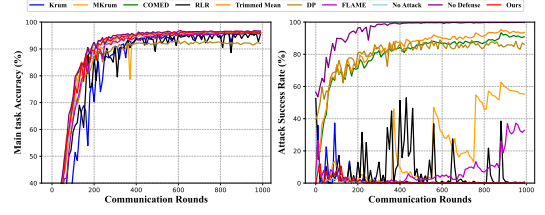


(c)  $\alpha = 0.5$

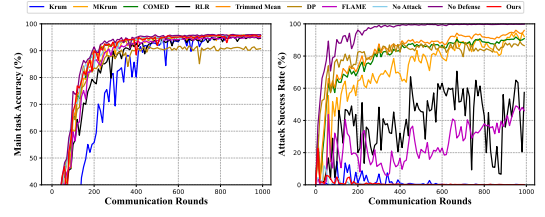


(d)  $\alpha = 0.1$

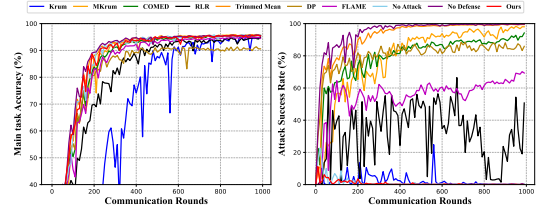
Fig. 8. CIFAR-100



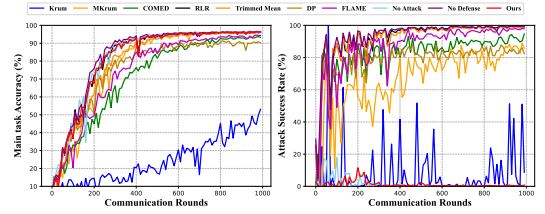
(a) IID



(b)  $\alpha = 1$



(c)  $\alpha = 0.5$



(d)  $\alpha = 0.1$

Fig. 9. GTSRB